JACS
JOURNAL OF THE AMERICAN CHEMICAL SOCIETY
Article
pubs.acs.org/JACS

Electronic and Optical Properties of Methylated Adamantanes

Torbjörn Rander,* Tobias Bischoff, Andre Knecht, David Wolter, Robert Richter, Andrea Merli, and Thomas Möller

Technische Universität Berlin, Hardenbergstr. 36, 10623 Berlin, Germany

ABSTRACT: Recent theoretical work has identified functionalized diamondoids as promising candidates for the tailoring of fluorescent nanomaterials. However, experiments confirming that optical gap tuning can be achieved through functionalization have, up until now, found only systems where fluorescence is quenched. We address this shortcoming by investigating a series of methylated adamantanes. For the first time, a class of functionalized diamondoids is shown to fluoresce in the gas phase. In order to understand the evolution of the optical and electronic structure properties with degree of functionalization, photoelectron spectroscopy was used to map the occupied valence electronic structure, while absorption and fluorescence spectroscopies yielded information about the unoccupied electronic structure and postexcitation relaxation behavior. The resulting spectra were modeled by (time-dependent) density functional theory. These results show that it is possible to overcome fluorescence quenching when functionalizing diamondoids and represent a significant step toward tailoring the electronic structure of these and other semiconductor particles in a manner suitable to applications.

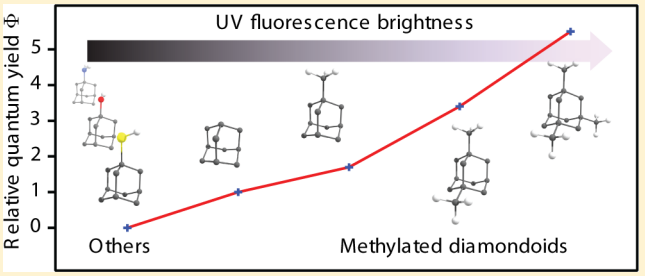

INTRODUCTION

The search for fluorescent nanomaterials is a highly active research area, where uses, including, for example, as textile colors, printing inks, fluorescent tags,[1−4] and in the security area, drive development. The rationale behind moving from molecular dyes to nanomaterials is that such applications can all benefit from taking advantage of the special properties of nanoparticles, such as their size-dependent absorption and emission wavelengths, and ability to be chemically functionalized. For many purposes, however, issues with biocompatibility, photostability and chemical inertness limit the usefulness of most nanoparticle based dyes. Recently, theoretical predictions have identified functionalized diamondoids as a class of nanomaterials that could overcome many of these limitations, while offering band gap tuning possibilities from the infrared to ultraviolet.[5]

Diamondoids[6] are hydrogen terminated sp^3-hybridized nanocarbons, congruent with the diamond lattice, different from the sp^2-hybridized nanocarbons, which include the fullerenes,[7] graphene,[8] and carbon nanotubes.[9] Together, they comprise a large and growing global market, and already find applications in fields ranging from biomedicine[10] to quantum information processing.[11] The diamondoids have become widely available for study during the last 10 years through novel isolation[12] and synthesis schemes.[13] They have attracted a lot of attention due to the properties they share with bulk diamond, e.g., their superb chemical and mechanical stability,[14] and due to a unique combination of intrinsic physical properties such as UV fluorescence,[15] negative electron affinity,[16] and perfect shape and size selectability. The last point in particular makes them ideal benchmark systems for studying physics in the size region where the molecular and solid state descriptions start to overlap.[17]

It is possible to modify the diamondoids chemically through functionalization (replacement of a surface hydrogen by a functional group),[18] doping (replacement of a cage carbon with a noncarbon atom),[19] and through electronic blending (the replacement of a surface hydrogen by an unsaturated hydrocarbon containing sp^2-hybridized carbon atoms).[20] All of these modifications influence the electronic structure of the precursor diamondoid, and it is possible to choose them such as to tune, e.g., the optical gap[5] or the ionization potential (IP).[21] This leads to a large parameter space when considering diamondoids for applications, which have been recently explored in the contexts of electron emitting coatings,[22] single particle rectification,[23] and self-assembled nanowires.[24] Fluorescence, however, has been shown to be quenched in all functionalized diamondoids investigated to date.[25]

In this work, we investigate a type of functionalized diamondoids where the electronic structures can be said to be extensions to their pristine counterparts, namely methylated adamantanes, and characterize their optical and (valence) electronic structure properties. All investigated members of this class of functionalized diamondoids are shown to fluoresce, with higher quantum yields than their pristine counterparts.

EXPERIMENTAL AND COMPUTATIONAL DETAILS

We investigated the following, commercially available samples: adamantane (Sigma-Aldrich, purity ≥99%), 1-methyladamantane (Alinda Chemical, purity ≥99%), 1,3-dimethyladamantane (Sigma-

Received: May 18, 2017
Published: July 24, 2017

DOI: 10.1021/jacs.7b05150
J. Am. Chem. Soc. 2017, 139, 11132−11137

Aldrich, purity ≥99%) and 1,3,5-trimethyladamantane (Alinda Chemical, purity ≥98%). All measurements were performed in the gas phase. The investigated compounds all had sufficiently high vapor pressures that no additional heating was required. We recorded valence photoelectron spectra using an effusive jet source and a Scienta SES-2002 hemispherical analyzer in conjunction with a SPECS 10/35 He-lamp (21.22 eV photons). The total experimental resolution in these measurements was 30 meV. Chamber pressures during measurements were around 6×10^{-6} mbar, 1 order of magnitude higher than the background pressure. Absorption, fluorescence and radiative rate measurements were performed at the U125/2 NIM beamline at the BESSY II synchrotron facility of the Helmholtz-Zentrum Berlin, Germany. Absorption was recorded by a photodiode mounted at the exit window of a 10 cm single-pass multipurpose gas cell. Simultaneously, a perpendicularly mounted fast photomultiplier tube (Hamamatsu R7400P-06) recorded the fluorescence yield, and radiative rates were measured by single-photon counting using a FastCard P7887 Multiscaler. Fluorescence emission spectra were recorded using an Andor Shamrock SR-303i spectrometer mounted across from the photomultiplier tube, with a 1200 lines/mm grating, and a cooled CCD camera at −100 °C. An entrance slit of 20 μm was used, which resulted in a resolution of about 4 meV at the center energy of 5.5 eV.

In order to understand the observed spectral shapes, we performed density functional theory (DFT, photoelectron spectra, ground state geometries and frequencies) and time dependent density functional theory (TDDFT, excited state geometries and frequencies) computations using Gaussian 09.[26] Since our samples were electronically extended diamondoids, we limited the calculations to the use of the B3LYP functional[27,28] in the case of photoionization, and the long-range corrected CAM-B3LYP[29] functional for the optical spectra. A 6-311++G** basis set[30] was sufficient for a good match between theory and experiment. These functionals and basis set have been shown to describe the (larger) pristine diamondoids well.[31] In order to calculate the ionization potentials E_I, the total energies of the particles in their ground and ionic states were subtracted such that $E_I = |E_{sample} - E^+_{sample}|$. The photoelectron spectra were treated within the Franck–Condon approximation,[32,33] including Duschinsky rotation and shifts,[34] and vibrational stick spectra were convolved with a Gaussian broadening matching the experimental resolution. In the case of absorption and fluorescence spectra, an approach similar to the one followed for pristine diamondoids in previous work[31,35] was used, including a Herzberg–Teller[36] treatment. The calculated vibrational envelopes were shifted in energy to match the experimental data, and for the fluorescence spectra, the energy axis was scaled by a factor 0.98 to match the experiment.

RESULTS AND DISCUSSION

Figure 1 shows valence photoelectron spectra from pristine adamantane and from all methylated adamantanes. The diamondoid structures are depicted without their hydrogen atoms throughout the manuscript. The calculated vibrational spectra stemming from the photoionization $C_{10}H_{16-N}(CH_3)_N + \hbar\omega \rightarrow C_{10}H_{16-N}(CH_3)^+_N + e^-$ of the highest occupied molecular orbitals (HOMOs) are also shown. The valence photoelectron spectra of adamantane and diamantane were recently investigated theoretically by Gali et al.[37] It was determined that overall, photoelectron line-shapes in diamondoids cannot be fully understood within the electron quasi-particle picture. Using a many-body perturbation theory (MBPT) approach, the authors showed that strong electron-vibrational coupling induces satellite structures in the valence photoelectron features. However, the fine-structure in the valence features could not be explained within that theoretical framework. For adamantane, such a satellite is predicted to lie around $E_S \simeq 10$ eV, where, in the quasi-particle picture, there is no energy level. In our experimental spectra, this feature can be seen as a shoulder around 9.9 eV, not only in adamantane but also in all of the methylated species. It is also immediately apparent that the spectral shapes from the methylated species are smoother than those of adamantane, which shows pronounced fine-structure. The ionization potential difference is roughly ΔE_I = 50 meV per added methyl group (see Table 1). The trend toward lower ionization potential for larger systems can be explained through additional screening of the valence hole due to the added methyl groups. The vibrational calculations, based on a pure Franck–Condon approach, show remarkable agreement with the experimental spectra, especially in the case of adamantane. The difference between experiments and calculations for the methylated samples are due to the low rotational barriers of the added methyl groups (≃0.1 eV). Thus, the geometrical changes between ground and ionic state are not perfectly represented by the difference between the 0 K structures. Even so, these findings show that the adiabatic approach is quite accurate for determining vibrational fine-structure in (methylated) diamondoids, and that a combination of the MBPT and adiabatic approaches could feasibly describe such systems well.

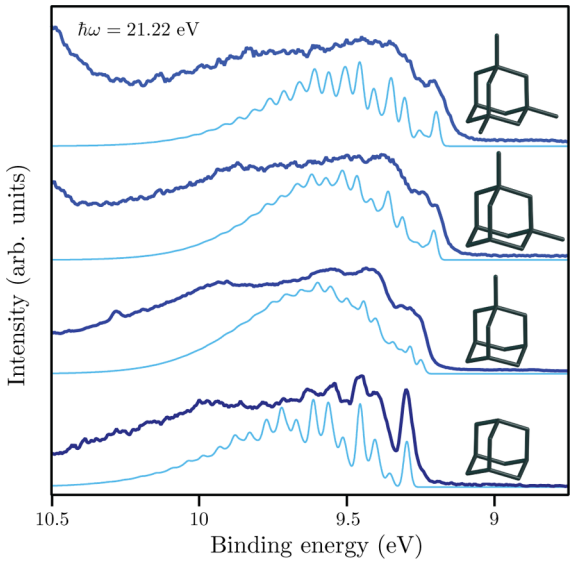

Figure 1. Valence photoelectron spectra (solid, dark blue lines) of pristine adamantane (bottom) and the methylated adamantanes. The thin, light blue lines show the calculated vibrational envelope of the HOMO photoionization, with a Gaussian broadening of 25 meV.

Table 1. Experimental and Calculated Ionization Potentials of the Methylated Adamantane Series

sample	exp. IP (eV)	theo. IP (eV)
adamantane	9.23(1)[38]	9.28,[39] 9.32[40]
1-methyladamantane	9.19(1)	8.97
1,3-dimethyladamantane	9.14(2)	8.94
1,3,5-trimethyladamantane	9.09(1)	8.91

Figure 2 shows the UV absorption spectra of pristine and methylated adamantanes. Although the spectra share many similarities with the one of pristine diamondoids, there is one surprising trend when methyl groups are added. In pristine diamondoids, optical gaps[41] have been shown to decrease monotonically with increasing size, which fits well into the framework of quantum confinement.[17] Table 2 shows the measured state energies. For methylated adamantane, the

DOI: 10.1021/jacs.7b05150
J. Am. Chem. Soc. 2017, 139, 11132–11137

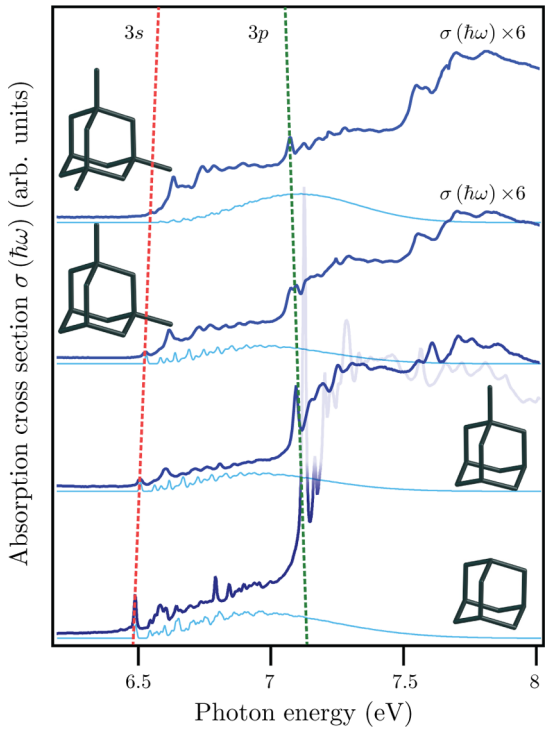

Figure 2. Absorption spectra from pristine and methylated adamantanes (solid, dark blue lines) and the calculated vibrational envelopes (thin, light blue lines, convolved with a Gaussian broadening of 12 meV) of the corresponding $S_0 \rightarrow S_1$ transitions. The red dashed line indicates the shift in 3*s* energy, while the green dashed line indicates the shift in 3*p* energy. The upper two experimental absorption spectra have been scaled for presentation purposes.

Table 2. Measured Energy of 3*s* and 3*p* Rydberg-like States in Pristine and Methylated Adamantanes

sample	3*s* (eV)	3*p* (eV)
adamantane	6.49(1)	7.13(1)
1-methyladamantane	6.51(1)	7.10(1)
1,3-dimethyladamantane	6.53(2)	7.08(2)
1,3,5-trimethyladamantane	6.55(2)	7.07(2)

lowest energy feature (a 3*s* Rydberg-like state at 6.49 eV for adamantane[42]) is present in all spectra, but shifts toward higher energy with the addition of methyls. This would seem to contradict quantum confinement, since with each extra methyl, the particle grows. For the 3*p* Rydberg-like state found at 7.13 eV in adamantane, the situation is reversed, as it shifts down in energy with an increased number of methyls. We propose that this is due to the fact that in this case at the molecular limit, the confining entities are the Rydberg-like orbitals, rather than the whole particle. While in adamantane, the 3*s* orbital is delocalized over the surface H atoms, the corresponding orbitals in methylated species are, effectively, reduced in volume by the addition of methyl groups, since these protrude through the 3*s* orbitals. Figure 3 shows a comparison between the lowermost unoccupied molecular orbitals (LUMOs) of pristine and methylated adamantanes, where this can be clearly seen. In contrast, the larger LUMO+1 3*p* orbitals are not penetrated by the methyl groups. Hence, the 3*p* Rydberg features shift with particle size as intuitively predicted by quantum confinement, while the 3*s* Rydberg features do not. This is a very clear illustration that even though the quantum

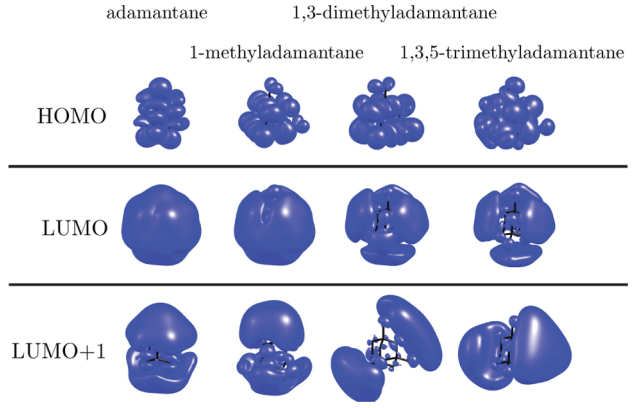

Figure 3. Outer valence orbitals of pristine adamantane (left) and methylated adamantanes, degree of methylation ascending from left to right. The localization of the HOMO to the cage structure, as well as the Rydberg character of the LUMO and LUMO+1 states can be seen. The protrusion of the methyl groups through the LUMO is clearly visible.

confinement model is applicable when describing the optical gaps in pristine diamondoids, care has to be taken when dealing with molecular systems where the degree of electron delocalization is sometimes counterintuitive.

Like the pristine diamondoids, the methylated diamondoids we investigated fluoresce. To our knowledge, these are the first functionalized diamondoids to do so. Usually, in diamondoid derivatives, examples being thiols, alcohols and amines, fluorescence is quenched by the addition of one or more functional groups.[25] Figure 4 shows the fluorescence emission spectra of methylated diamondoids, excited at the 3*s* resonances from Table 2. The respective excited state structures can be seen on the left of the figure. The spectra show marked similarity to the pristine adamantane, and all stem from $S_0 \leftarrow S_1$ fluorescence. Overall, the spectral envelope looks smoother the more methyls are added, which is due to the increased number of degrees of rotational and vibrational freedom contributing to spectral congestion through internal vibrational redistribution (IVR) and internal conversion, and in the case of 1,3,5-trimethyladamantane also from a significant geometrical change between the ground and excited state. As is the case for pristine diamondoids, the photophysics can be understood in the Franck−Condon picture, including the Herzberg−Teller term in the transition dipole matrix elements,[31] except in the case of 1,3,5-trimethyladamantane. For the latter, significant non-Born−Oppenheimer effects play a role, due to the breaking of a C−C bond between the 5 and 6 positions (calculated $r_{5-6}(S_0) = 1.55$ Å $\rightarrow r_{5-6}(S_1) = 1.80$ Å) in the diamondoid cage upon photoexcitation. The fact that this absorption spectrum has very sharp features while the corresponding fluorescence emission spectrum is featureless indicates that the rearrangement is a fairly slow process, taking place between photoexcitation and fluorescence relaxation. This is also manifested in the calculated fluorescence emission spectra through very low predicted Franck−Condon (FC) factors compared to what is observed experimentally. The theoretically computed frequencies, however, match the experimental spectra well, and scaled FC factors show good agreement to the experiment.

The main pane of Figure 5 shows the relative fluorescence quantum yields $\Phi(\hbar\omega)$, calculated by $\Phi(\hbar\omega) = I_{emi}(\hbar\omega)/\sigma(\hbar\omega)$, where $I_{emi}(\hbar\omega)$ is the fluorescence yield and $\sigma(\hbar\omega)$ is the absorption cross section. The inset shows the fluorescent

DOI: 10.1021/jacs.7b05150
J. Am. Chem. Soc. 2017, 139, 11132−11137

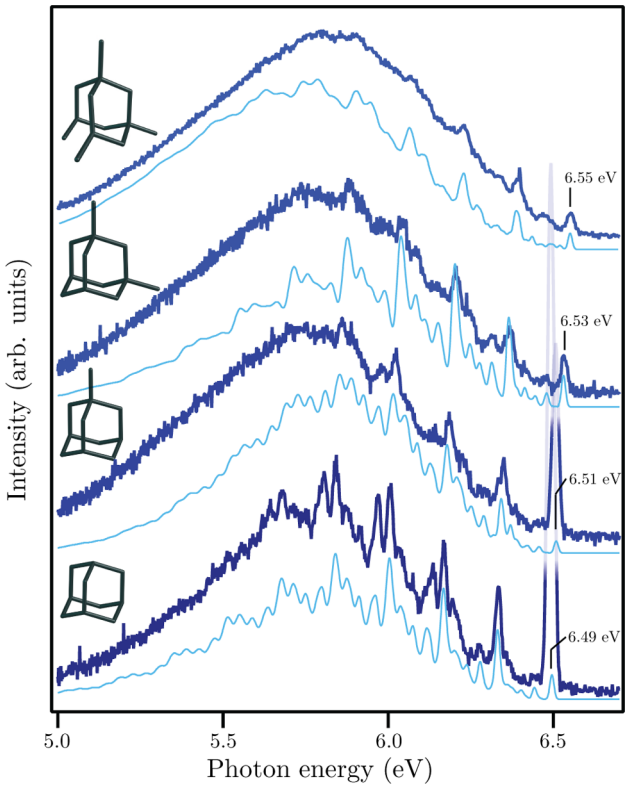

Figure 4. Fluorescence emission spectra of pristine and methylated adamantanes (dark blue lines) and the calculated vibrational envelopes (thin, blue lines, convolved with a 12 meV fwhm Gaussian) of the corresponding $S_0 \leftarrow S_1$ transitions. The excited state structures are shown on the left, and the excitation energies marked on the right side.

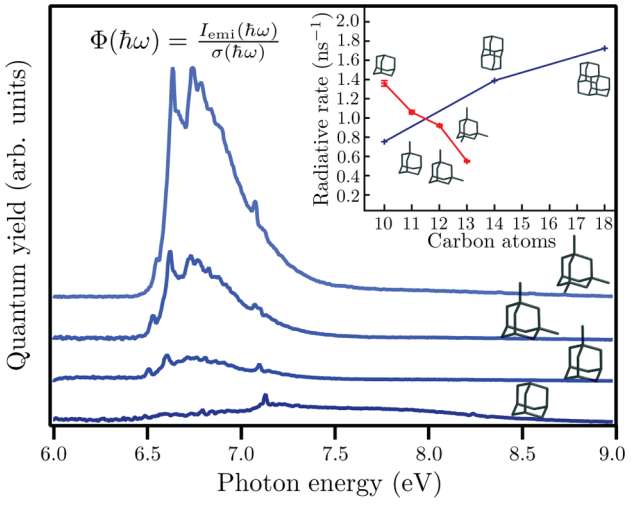

Figure 5. Relative fluorescence quantum yields, emission between 5.0 and 6.5 eV (main) of methylated adamantanes and fluorescent rates (inset) of the lower diamondoids (blue curve from ref 35) and methylated adamantanes (red curve this work).

rates of methylated adamantanes and of the lower diamondoids. The region between 6.5 and 7.1 eV contains only excitations to vibrational overtones in the 3*s* Rydberg-like state.[42] As can be seen, Φ increases drastically in this energy range the more methyls are added. This implies that the addition of specific functional groups might facilitate IVR in such a way that more quanta end up in optically active normal modes. It can also be seen that in comparison with pristine diamondoids, there is a significant difference in how the fluorescent rate of methylated diamondoids develops with size. Where, in pristine diamondoids, the rate increases with size, in the methylated adamantanes, the trend is reversed. The addition of a methyl group decreases the fluorescent rate by 0.20 ns^{-1} on average (see Table 3). Still, both internal conversion and IVR processes take place on faster time-scales (ps) than fluorescence (ns). Thus, the radiative decays all stem from $S_0 \leftarrow S_1$ as is the case in pristine diamondoids, but with a higher quantum yield[15] and a longer radiative lifetime. A key commonality between methylated adamantanes and pristine diamondoids is that the HOMO is localized to the carbon cage, whereas the LUMO is delocalized over the surface hydrogens of the cage. We tentatively attribute the fact that fluorescence is enhanced rather than quenched in methylated diamondoids to this fact, and to the confinement of the 3*s*-excited state electron with the addition of the functional groups. This identifies a key question for the future design of fluorescent functionalized diamondoids, namely if this is a general trend, and if it is possible to achieve fluorescence in a particle where the HOMO is localized to the functional group, as is most often the case.

Table 3. Relative Fluorescence Quantum Yield and Fluorescent Rates of Pristine and Methylated Adamantanes Excited at the 3*s* Resonance[a]

sample	Φ (3*s*)	Γ_{rad} (ns^{-1})
adamantane	0.010[15]	1.35(3), 0.75[35]
1-methyladamanantane	0.017	1.06(2)
1,3-dimethyladamantane	0.034	0.92(1)
1,3,5-trimethyladamantane	0.055	0.55(1)

[a]The difference between the radiative rate for adamantane measured in this work and in the work by Richter et al.[35] is due to the use of an improved detector system, where systematic errors have been significantly reduced.

CONCLUSIONS

We investigated the electronic structure in a series of functionalized diamondoid derivatives, namely methylated adamantanes. Valence photoelectron spectra show that the shift in the HOMO energy with size can be explained straightforwardly by screening induced by addition of methyl groups. The trend in LUMO energies, at first glance, contradicts the quantum confinement model. However, careful consideration of how the LUMO develops with particle size leads to the conclusion that there is no contradiction. The fluorescence of functionalized diamondoids was observed for the first time. The relative quantum yields and radiative rates of methylated adamantanes were determined. The former increase with the number of methyl groups, while the latter follow a decreasing trend with increasing particle size, completely reversed from the pristine diamondoids. We attribute the lack of fluorescence quenching in these systems to intact good spatial overlap of the carbon cage HOMO and hydrogen "shell" LUMO; in principle, the outer valence electronic structure resembles that of pristine diamondoids. The enhanced quantum yields and decreased radiative rates are attributed to more efficient intramolecular vibrational redistribution and to more confined excited state electrons in the methylated systems. The spectra were modeled using DFT and TDDFT. Including the Herzberg–Teller term in the transition dipole

DOI: 10.1021/jacs.7b05150
J. Am. Chem. Soc. 2017, 139, 11132–11137

matrix elements proved crucial to give a good agreement between experiment and theory. This comparison of a benchmark series of experiments and computations allows us to conclude that similar systems can, in most cases, be accurately described within the Franck−Condon−Herzberg−Teller framework. These findings provide impetus toward further investigations into which design parameters are important when looking at new candidate systems for tailored fluorescent properties in general, and specific guidelines for the design of fluorescent diamondoid derivatives. As such, they represent a landmark in the field, and pave the way for future optical applications of functionalized diamonoids.

AUTHOR INFORMATION

Corresponding Author

*torbjorn.rander@win.tu-berlin.de

ORCID

Torbjörn Rander: 0000-0003-4665-1215

Notes

The authors declare no competing financial interest.

ACKNOWLEDGMENTS

This study was funded by the Deutsche Forschungsgemeinschaft, DFG, through research unit FOR 1282, grant MO 719 10/1. We thank P. Baumgärtel for support during the synhcrotron beamtime, and the HZB for the allocation of synchrotron radiation beamtime.

REFERENCES

(1) Evanko, D. *Nat. Methods* **2008**, *5*, 218.
(2) Goncalves, T. M. S. *Chem. Rev.* **2009**, *109*, 190.
(3) Biju, V.; Itoh, T.; Anas, A.; Sujith, A.; Ishikawa, M. *Anal. Bioanal. Chem.* **2008**, *391*, 2469.
(4) Michalet, X.; Pinaud, F. F.; Bentolila, L. A.; Tsay, J. M.; Doose, S.; Li, J. J.; Sundaresan, G.; Wu, A. M.; Gambhir, S. S.; Weiss, S. *Science* **2005**, *307*, 538.
(5) Vörös, M.; Demjén, T.; Szilvási, T.; Gali, A. *Phys. Rev. Lett.* **2012**, *108*, 267401.
(6) Schwertfeger, H.; Fokin, A. A.; Schreiner, P. R. *Angew. Chem., Int. Ed.* **2007**, *47*, 1022.
(7) Kroto, H. W.; Heath, J. R.; O'Brien, S. C.; Curl, R. F.; Smalley, R. E. *Nature* **1985**, *318*, 162.
(8) Geim, A. K.; Novoselov, K. S. *Nat. Mater.* **2007**, *6*, 183.
(9) Sinnott, S. B.; Andrews, R. *Crit. Rev. Solid State Mater. Sci.* **2001**, *26*, 145.
(10) Reina, G.; Tamburri, E.; Orlanducci, S.; Gay, S.; Matassa, R.; Guglielmotti, V.; Lavecchia, T.; Terranova, M. L.; Rossi, M. *Biomatter* **2014**, *4*, e28537.
(11) Li, P.; Xiang, Z.; Rabl, P.; Nori, F. *Phys. Rev. Lett.* **2016**, *117*, 015502.
(12) Dahl, J. E.; Liu, S. G.; Carlson, R. M. K. *Science* **2003**, *299*, 96.
(13) Dahl, J. E.; Moldovan, J. M.; Wei, Z.; Lipton, P. A.; Denisevich, P.; Gat, R.; Liu, S.; Schreiner, P. R.; Carlson, R. M. K. *Angew. Chem., Int. Ed.* **2011**, *49*, 9881.
(14) Raty, J.; Galli, G. *Nat. Mater.* **2003**, *2*, 792.
(15) Landt, L.; Kielich, W.; Wolter, D.; Ehresmann, A.; Möller, T. *Phys. Rev. B: Condens. Matter Mater. Phys.* **2009**, *80*, 205323.
(16) Drummond, N. D.; Williamson, A. J.; Needs, R. J.; Galli, G. *Phys. Rev. Lett.* **2005**, *95*, 096801.
(17) Willey, T. M.; Bostedt, C.; van Buuren, T.; Dahl, J. E.; Liu, S. G.; Carlson, R. M. K.; Terminello, L. J.; Möller, T. *Phys. Rev. Lett.* **2005**, *95*, 113401.
(18) Kahl, P.; Tkachenko, B. A.; Novikovsky, A. A.; Becker, J.; Dahl, J. E.; Carlson, R. M. K.; Fokin, A. A.; Schreiner, P. R. *Synthesis* **2014**, *46*, 787.
(19) Fokin, A. A.; Zhuk, T. S.; Pashenko, A. E.; Dral, P. O.; Gunchenko, P. A.; Dahl, J. E.; Carlson, R. M. K.; Koso, T. V.; Serafin, M.; Schreiner, P. R. *Org. Lett.* **2009**, *11*, 3068.
(20) Fokin, A. A.; Chernish, L. V.; Gunchenko, P. A.; Tikhonchuk, E. Y.; Hausmann, H.; Serafin, M.; Dahl, J. E.; Carlson, R. M. K.; Schreiner, P. R. *J. Am. Chem. Soc.* **2012**, *134*, 13641.
(21) Rander, T.; Staiger, M.; Richter, R.; Zimmermann, T.; Landt, L.; Wolter, D.; Dahl, J. E.; Carlson, R. M. K.; Tkachenko, B. A.; Fokina, N. A.; Schreiner, P. R.; Möller, T.; Bostedt, C. *J. Chem. Phys.* **2013**, *138*, 024310.
(22) Narasimha, K. T.; Ge, C.; Fabbri, J. D.; Clay, W.; Tkachenko, B. A.; Fokin, A. A.; Schreiner, P. R.; Dahl, J. E.; Carlson, R. M. K.; Shen, Z. X.; Melosh, N. A. *Nat. Nanotechnol.* **2016**, *11*, 267.
(23) Randel, J. C.; Niestemski, F. C.; Botello-Mendez, A. R.; Mar, W.; Ndabashimiye, G.; Melinte, S.; Dahl, J. E. P.; Carlson, R. M. K.; Butova, E. D.; Fokin, A. A.; Schreiner, P. R.; Charlier, J.-C.; Manoharan, H. C. *Nat. Commun.* **2014**, *5*, 4877.
(24) Yan, H.; Hohman, J. N.; Li, F. H.; Jia, C.; Solis-Ibarra, D.; Dahl, J. E. P.; Carlson, R. M. K.; Tkachenko, B. A.; Fokin, A. A.; Schreiner, P. R.; Liang, Y.; Kim, T. R.; Devereaux, T.; Shen, Z.-X.; Melosh, N. A. *Nat. Mater.* **2017**, *16*, 349.
(25) Landt, L.; Staiger, M.; Wolter, D.; Klünder, K.; Zimmermann, P.; Willey, T. M.; van Buuren, T.; Brehmer, D.; Schreiner, P. R.; Thkachenko, B. A.; Fokin, A. A.; Möller, T.; Bostedt, C. *J. Chem. Phys.* **2010**, *132*, 024710.
(26) Frisch, M. J.; Trucks, G. W.; Schlegel, H. B.; Scuseria, G. E.; Robb, M. A.; Cheeseman, J. R.; Scalmani, G.; Barone, V.; Mennucci, B.; Petersson, G. A.; Nakatsuji, H.; Caricato, M.; Li, X.; Hratchian, H. P.; Izmaylov, A. F.; Bloino, J.; Zheng, G.; Sonnenberg, J. L.; Hada, M.; Ehara, M.; Toyota, K.; Fukuda, R.; Hasegawa, J.; Ishida, M.; Nakajima, T.; Honda, Y.; Kitao, O.; Nakai, H.; Vreven, T.; Montgomery, J. A., Jr.; Peralta, J. E.; Ogliaro, F.; Bearpark, M.; Heyd, J. J.; Brothers, E.; Kudin, K. N.; Staroverov, V. N.; Kobayashi, R.; Normand, J.; Raghavachari, K.; Rendell, A.; Burant, J. C.; Iyengar, S. S.; Tomasi, J.; Cossi, M.; Rega, N.; Millam, J. M.; Klene, M.; Knox, J. E.; Cross, J. B.; Bakken, V.; Adamo, C.; Jaramillo, J.; Gomperts, R.; Stratmann, R. E.; Yazyev, O.; Austin, A. J.; Cammi, R.; Pomelli, C.; Ochterski, J. W.; Martin, R. L.; Morokuma, K.; Zakrzewski, V. G.; Voth, G. A.; Salvador, P.; Dannenberg, J. J.; Dapprich, S.; Daniels, A. D.; Farkas; Foresman, J. B.; Ortiz, J. V.; Cioslowski, J.; Fox, D. J. *Gaussian 09*, Revision D.01; Gaussian Inc.: Wallingford, CT, 2009.
(27) Becke, A. D. *J. Chem. Phys.* **1993**, *98*, 5648.
(28) Stephens, P. J.; Devlin, F. J.; Chabalowski, C. F.; Frisch, M. *J. Phys. Chem.* **1994**, *98*, 11623.
(29) Yanai, T.; Tew, D. P.; Handy, N. C. *Chem. Phys. Lett.* **2004**, *393*, 51.
(30) Krishnan, R.; Binkley, J. S.; Seeger, R.; Pople, J. A. *J. Chem. Phys.* **1980**, *72*, 650.
(31) Richter, R.; Röhr, M. I. S.; Zimmermann, T.; Petersen, J.; Heidrich, C.; Rahner, R.; Möller, T.; Dahl, J. E.; Carlson, R. M. K.; Mitric, R.; Rander, T.; Merli, A. *Phys. Chem. Chem. Phys.* **2015**, *17*, 4739.
(32) Franck, J.; Dymond, E. G. *Trans. Faraday Soc.* **1926**, *21*, 536.
(33) Condon, E. U. *Phys. Rev.* **1928**, *32*, 858.
(34) Duschinsky, F. *Acta Physicochim. URSS* **1937**, *7*, 551.
(35) Richter, R.; Wolter, D.; Zimmermann, T.; Landt, L.; Knecht, A.; Heidrich, C.; Merli, A.; Dopfer, O.; Reiß, P.; Ehresmann, A.; Petersen, J.; Dahl, J. E.; Carlson, R. M. K.; Bostedt, C.; Möller, T.; Mitric, R.; Rander, T. *Phys. Chem. Chem. Phys.* **2014**, *16*, 3070.
(36) Azumi, T.; Matsuzaki, K. *Photochem. Photobiol.* **1977**, *25*, 315.
(37) Gali, A.; Demján, T.; Vörös, M.; Thiering, G.; Cannuccia, E.; Marini, A. *Nat. Commun.* **2016**, *7*, 11327.
(38) Lenzke, K.; Landt, L.; Hoener, M.; Thomas, H.; Dahl, J. E.; Liu, S. G.; Carlson, R. M. K.; Möller, T.; Bostedt, C. *J. Chem. Phys.* **2007**, *127*, 084320.
(39) Fokin, A. A.; Tkachenko, B. A.; Gunchenko, P. A.; Gusev, D. V.; Schreiner, P. R. *Chem. - Eur. J.* **2005**, *11*, 7091.

DOI: 10.1021/jacs.7b05150
J. Am. Chem. Soc. 2017, 139, 11132−11137

(40) Zimmermann, T.; Richter, R.; Knecht, A.; Fokin, A. A.; Koso, T. V.; Chernish, L. V.; Gunchenko, P. A.; Schreiner, P. R.; Möller, T.; Rander, T. *J. Chem. Phys.* **2013**, *139*, 084310.
(41) Landt, L.; Klünder, K.; Dahl, J. E.; Carlson, R. M. K.; Möller, T.; Bostedt, C. *Phys. Rev. Lett.* **2009**, *103*, 047402.
(42) Raymonda, J. W. *J. Chem. Phys.* **1972**, *56*, 3912.

DOI: 10.1021/jacs.7b05150
J. Am. Chem. Soc. 2017, 139, 11132−11137